PHYSICAL REVIEW B VOLUME 24, NUMBER 11 1 DECEMBER 1981

Atomic ordering transition in FeCo

Ben deMayo
Department of Physics, West Georgia College, Carrollton, Georgia 30118
(Received 6 April 1981)

Atomic ordering in equiatomic iron-cobalt was investigated using Mössbauer spectroscopy of quenched samples. The order-disorder transition at 730 °C and the "550 °C anomaly" were observed. A statistical phenomenological model was used to determine the temperature dependence of the short-range order parameter; the critical index β was found to be 0.324 ± 0.016.

I. INTRODUCTION

Much progress has been made over the past 15 years in the understanding of phase transitions and critical phenomena. A classic example of such a transition is the atomic ordering of equiatomic iron-cobalt (FeCo) into the cesium chloride structure below 730 °C.[1]

In this study, the Mössbauer effect was used to investigate FeCo samples quenched from various temperatures. Neutron diffraction confirmed the state of long-range order in two samples. Previous Mössbauer work on iron-cobalt has included studies at temperature,[2–4] studies of quenched samples of 30–70% cobalt,[5,6] studies of both quenched and heated samples,[7] and secondary electron spectroscopy of films.[8]

The Mössbauer effect can yield information pertinent to our understanding of phase transitions.[9] The measured magnetic hyperfine field, H, of a sample is the composite of the hyperfine field of all of the ^{57}Fe nuclei of the sample. Atomic ordering changes the local atomic environment of each iron atom, and if short-range effects on the hyperfine field are present, these will manifest themselves both as changes in the overall field H and changes in the shapes of the Mössbauer absorption lines. The isomer shift, which is a reflection of the electric charge density at the ^{57}Fe nuclei, and the quadrupole splitting, which is due to the electric field gradient at the ^{57}Fe nuclei, might be expected to be somewhat insensitive to atomic ordering in metallic alloys.

The Mössbauer parameters can be used to determine the temperature dependence of the atomic ordering parameter and then to calculate the critical exponent β of the order-disorder transition.[10] This exponent has been obtained theoretically from the three-dimensional Ising model by a number of different approaches, including using variational approximations for renormalization-group transformations,[11] the n-vector model through field theoretical methods (the asymptotic estimate of the behavior of perturbation series at large orders),[12] and an analysis of the high-temperature series expansion.[13] A favorable comparison between the experimental and theoretical values of β would help further substantiate the important concepts of the universality of phase transitions and of scaling relations.[10]

II. EXPERIMENTAL

Conventional techniques were used to prepare the samples, obtain Mössbauer spectra, and analyze the results.[6] Required proportions of high purity (99.999%) iron and cobalt were arc melted and then homogenized at 1200 °C for 1 week in vacuum. Powders of 0.07 mm or less diameter were mechanically ground from the ingots and subsequently heat treated. Samples then were fast quenched into ice-water from temperatures ranging from 850 to 510 °C. The quench temperature was reached by first heating the sample to 500 °C in hydrogen for about 1 h. Then the temperature was raised to 850 °C and lowered in steps of increasing time to the desired quench temperature. More than 2 weeks were required to reach the 510 °C quench temperature. One sample ("annealed") was furnace cooled after 50 h at 500 °C; another ("ground") was kept in the as-ground condition. Mössbauer absorbers were prepared by pressing the powders into pellets with LiOH.

All Mössbauer spectra were taken at room temperature with a conventional constant acceleration drive. The ^{57}Co source was diffused into copper to produce a single emission line. Calibration spectra of an enriched ^{57}Fe foil were taken before and after each sample run. This foil was in turn calibrated against a sodium nitroprusside standard absorber. A least-squares fit to six lines was performed for each run using a computer; from these the Mössbauer parameters were determined: H, the magnetic hyperfine field at the ^{57}Fe nuclei; IS, the isomer shift; QS, the quadrupole splitting; and HWHM, the half-width at half maximum of each absorption line.

Neutron diffraction was used to determine the long-range order parameter, S, of the sample as-ground ($S \leq 0.08 \pm 0.04$) and of the annealed sample

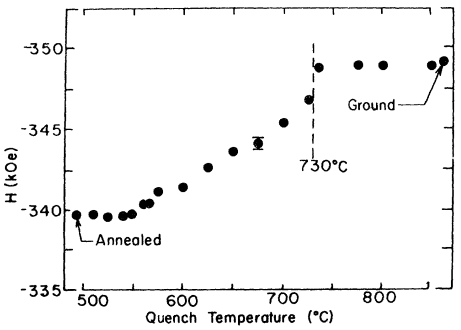

FIG. 1. Magnetic hyperfine field, H, at the ^{57}Fe nuclei in FeCo vs temperature of the sample just before quenching into ice water. Also shown are H for a sample annealed at 500 °C ("annealed") and for a sample ground into powder but not heat treated ("ground"). All of the errors are smaller than the data points except for the single point shown with error bars.

($S = 0.87 \pm 0.04$). Pure iron powders were heat-treated, quenched, and made into pellets in the same manner as the alloy samples; none showed any resulting effects in their Mössbauer parameters.

III. RESULTS

The dependence on quench temperature of the Mössbauer parameters revealed several interesting features. As shown in Fig. 1, H increases with increasing quench temperature up to about 730 °C then it levels off. The order-disorder transition at 730 °C is clearly evident. Furthermore, the annealed sample has an H close to that of the samples quenched from low temperature, and the as-ground sample has an H close to that of the samples quenched from above the ordering temperature. The IS and QS are shown in Fig. 2 versus quench temperature. The order-dis-

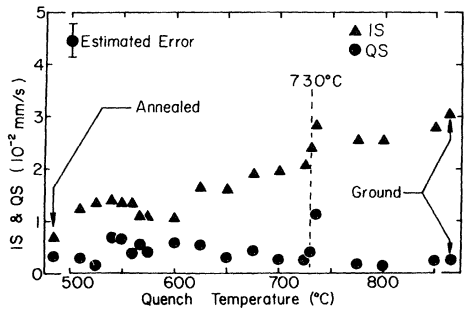

FIG. 2. Isomer shift, IS (triangles), and quadrupole splitting, QS (dots), of ^{57}Fe nuclei in Fe-Co vs the temperature of the sample just before quenching into ice water. The typical estimated error is also shown.

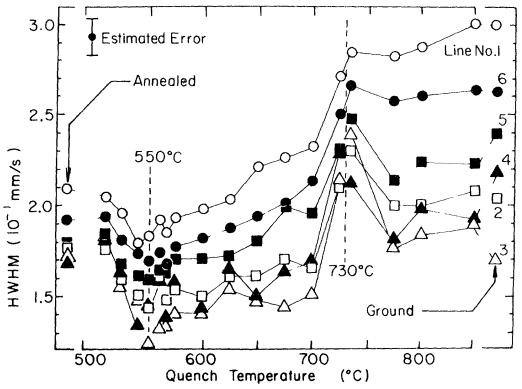

FIG. 3. Half linewidths at half maximum, HWHM, for the six Mössbauer absorption lines vs the temperature of the sample just before it was quenched into ice water. Line numbers (No.1 = lowest energy) are given on the right. Solid lines connect the points to assist in visualizing the results. The typical estimated error is also shown.

order transition is only mildly evident in IS and not at all QS. A more interesting set of data is shown in Fig. 3 for the HWHM of the six lines versus quench temperature. Here the order-disorder transition is evident, as is the "550 °C anomaly."[14–17] Note that the lines are narrower for samples quenched from 550 °C than they are for the annealed sample. The small differences in HWHM between lines 1 and 6, 2 and 5, and 3 and 4 were not observed in pure iron samples, but this effect has been noted in FeCo by other workers.[8]

IV. DISCUSSION

The results can be related to current theories of critical phenomena by using them to find the dependence of short-range order (SRO) on quench temperature. Assume that the measured changes of H are associated with local atomic environments. Then the SRO parameters $\{\alpha_i\}$ of Cowley[18] can give a quantitative description of the bcc alloy A_mB_{1-m}. The probabilities $\{p_i\}$ that any one of the c_i sites of the ith nearest-neighbor shell of an A atom is a B atom are known and the $\{\alpha_i\}$ are defined with respect to these probabilities. Upon inversion, the probabilities can be found from the $\{\alpha_i\}$

$$p_i = (1-m)(1-\alpha_i) \quad . \tag{1}$$

In a disordered alloy, all of the $\{\alpha_i\}$ are zero; in an ordered alloy, the $\{\alpha_i\}$ attain their maximum values, which depend on the composition m and shell i. The normalized SRO parameter $\alpha = \alpha_i/\alpha_{i,\max}$ is employed for convenience. The probability of finding exactly n_i B atoms among the c_i atoms in the ith shell around

an A atom is given by the binomial distribution

$$w_i(n_i) = \binom{c_i}{n_i} (p_i)^{n_i}(1-p_i)^{c_i-n_i} \quad . \tag{2}$$

In the case considered here, bcc $Fe_{50}Co_{50}$, only the first two normalized α_i's are used. Their temperature dependence is assumed to be the same and they are both characterized by the symbol "α." For the equiatomic alloy, Eq. (1) is

$$p_1 = (1+\alpha) \quad , \quad p_2 = (1-\alpha) \quad . \tag{3}$$

A phenomenological model based on the effect of cobalt neighbors on the effective field is useful:

$$H = H_0 + H_{NL} + n_1 H_1 + n_2 H_2 \quad , \tag{4}$$

where H_0 is the effective field in pure iron (−330.0 KOe), n_1 and n_2 are the number of cobalt first and second neighbors to the iron atom, H_1 and H_2 are the contributions of each cobalt first and second neighbor to H, and H_{NL} is the nonlocal contribution to H, in the sense that it is not dependent on local neighbor effects, but it does include the effect of changes in the magnetic moment at the given iron site. Note that additivity has been assumed; this is commonly done in dealing with dilute alloys and is sometimes used with concentrated alloys.[19] Equation (4) is the simplest expression possible which takes into account first and second near-neighbor effects and also nonlocal effects.

An experimental value for H is available for ordered and disordered samples between 30 and 70 at.% cobalt.[5] Since n_1 and n_2 are known for a particular composition at complete order and complete disorder, simultaneous equations can be set up to determine the unknown parameters H_1, H_2, and H_{NL}:

$$H^0 = H_0 + H_{NL}^0 + n_1^0 H_1^0 + n_2^0 H_2^0 \quad \text{(order)} \quad , \tag{5}$$

$$H^d = H_0 + H_{NL}^d + n_1^d H_1^d + n_2^d H_2^d \quad \text{(disorder)} \quad , \tag{6}$$

The unknown parameters may be obtained from the experimental data and Eqs. (5) and (6) with certain assumptions. If the parameters are assumed to be independent of atomic order, then the problem is reduced to solving for the three unknowns from two equations. A third relationship involving the parameters is obtained if the statistical ordering model is used with Eqs. (5) and (6) to calculate the linewidth of the absorption lines. The parameters H_{NL}, H_1, and H_2 may then be varied until the experimental linewidth agrees with the statistical model calculation. From Eqs. (5) and (6), two of the parameters H_{NL}, H_1, and H_2 are known as functions of the third. Figure 4 shows the calculated linewidth for the disordered $Fe_{50}Co_{50}$ case as a function of H_1, along with the experimentally observed HWHM. A unique

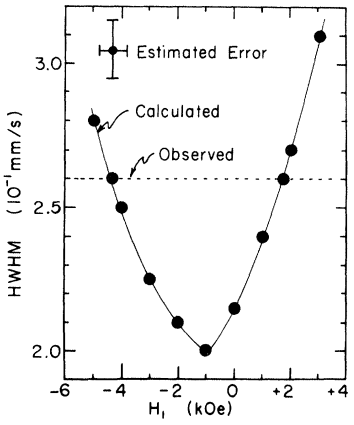

FIG. 4. Calculated HWHM for disordered FeCo vs the first-neighbor contribution H_1 of a cobalt atom. The observed value is also shown, as is the estimated error.

solution is not obtained; the two solutions which reproduce the HWHM data are ($H_1 = +4.3$ kOe, $H_2 = +2.7$ kOe, $H_{NL} = -44.1$ kOe) and ($H_1 = -1.7$ kOe, $H_2 = -5.3$ kOe, $H_{NL} = +3.9$ kOe). If it is further assumed that H_1 and H_2 are not dependent on composition, only the first solution can reproduce the measured H as a function of composition for both ordered and disordered samples. The positive sign of H_1 and H_2 of this solution infers a reduction in the magnitude of H for the addition of a first or second cobalt neighbor to the iron atom; the larger, negative value of H_{NL} may be associated with the dependence of H both on changes in the local iron moment and on a long-range effect. Any simplifications of Eq. (4) to include only two parameters leads to results which are conflicting and which cannot be used to reproduce the experimental linewidths.

This model of a neighbor-dependent effective magnetic field $H(n_1,n_2)$ for a particular iron atom now allows the use of the SRO parameter to calculate a Mössbauer spectrum. For each atomic configuration, the Mössbauer absorption lines are Lorentzian in shape and depend on the effective field of the atom according to

$$L_k(H) = \frac{1}{\pi G} \frac{1}{1 + \{[H_0 - H(n_1,n_2)]/G\}^2} \quad , \tag{7}$$

where k is an index for each of the six lines, and G is the HWHM of the line for a perfectly ordered sample. The observed absorption spectrum is a superposition of such lines. The calculation of a spectrum for a particular value of the SRO parameter involves summing over the possible near-neighbor configurations characterized by n_1 and n_2. One obtains for the

composite spectrum

$$L(H)=\frac{1}{\pi G}\sum_{k=1}^{6}c_k\sum_{n_1=0}^{8}\sum_{n_2=0}^{6}\left[\frac{w_1(n_1)w_2(n_2)}{1+\left[\frac{H_0-H(n_1,n_2)}{G}\right]^2}\right], \tag{8}$$

where c_k is a constant. H can be determined from the position of the center of one of these lines. The dependence of H on the SRO parameter enters the calculation through the probabilities of Eq. (3) and the binomial coefficients.

Figure 5 shows the calculated effective field versus the SRO parameter, α. The values of the solution of the phenomenological analysis above were used; however, the calculations were found to be not very sensitive to the particular values used. From the plot of H versus the SRO parameter and the plot of H versus quench temperature (Fig. 1), the dependence of the SRO parameter on temperature was deduced. This is shown in Fig. 6, along with neutron-diffraction results of Lyashenko[20] on the long-range order (LRO) parameter versus temperature.[21] The curve is drawn only to assist in viewing the data. Lyashenko's data had no error bars, and for a number of the circles (this work) the error bars are smaller than the circles. Table I contains the SRO parameter.

The results for the SRO parameter, α, were least-squares fitted using a computer to the reduced temperature, $x=(T_c-T)/T_c$, according to the power relation $\alpha=ax^b$. The values $a=2.64\pm0.13$ and $b=0.647\pm0.032$ were obtained with a goodness to fit parameter $P=0.974$ (a value of $P=1$ would indicate a perfect fit) if the 725°C data point was eliminated. Otherwise, the values were $a=2.10\pm0.10$, $b=0.532\pm0.026$, and $P=0.965$. This reflects the relative difficulty of obtaining a uniform, fast quench this close (5 °C) to the transition temperature. Figure 7 shows a log-log plot of the results; the straight line is the least-squares fitted relation. The placement of the 725 °C datum shows that short-range order characteristic of a lower temperature is probably present, as would be expected from a quench that was not fast and uniform. This lends justification to the omission of this point from the calculation of the values of a and b. Since the LRO parameter is proportional to the square root of the SRO parameter,[18] the value of the critical exponent is $\beta=0.324\pm0.016$.

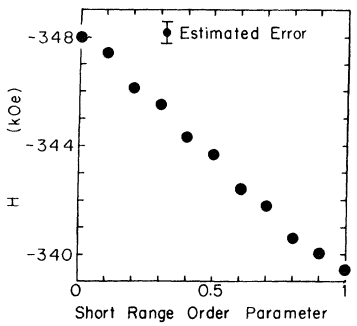

FIG. 5. Magnetic field, H, at ^{57}Fe nuclei vs normalized SRO parameter. Also shown is the typical estimated error.

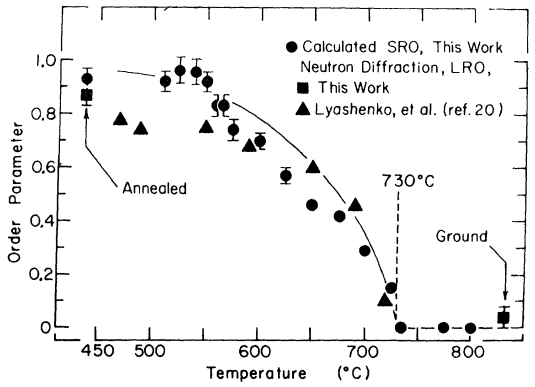

FIG. 6. Calculated normalized SRO parameter vs quench temperature (this work) and LRO parameter from neutron-diffraction results [this work and Lyashenko (Ref. 20)]. The solid line is given to assist in visualizing the results and does not represent any theory. No error bars were given by Lyashenko, and the error bars of the seven highest-temperature SRO values (dots) are smaller than the sizes of the dots.

TABLE I. Calculated short-range order parameter. (See also Fig. 6.)

Temperature just before fast quench (°C)	Short-range order parameter
500[a]	0.932 ±0.046
510	0.919 ±0.045
525	0.958 ±0.047
540	0.945 ±0.047
550	0.919 ±0.045
560	0.843 ±0.042
567	0.843 ±0.042
575	0.757 ±0.038
600	0.721 ±0.036
625	0.580 ±0.029
650	0.468 ±0.023
675	0.414 ±0.021
700	0.280 ±0.014
725	0.144 ±0.019
735–800	0

[a] Annealed.

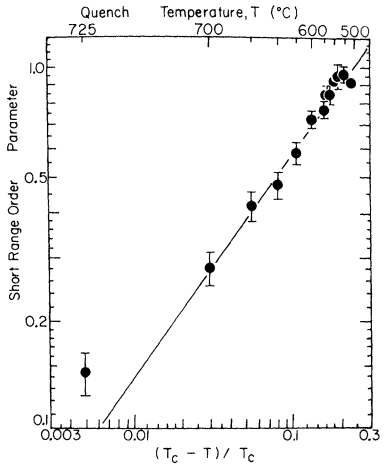

FIG. 7. Logarithmic plot of the SRO parameter vs the reduced temperature, $T' = (T_c - T)/T_c$. The straight line represents a least-squares fit of the data; a critical index $\beta = 0.324 \pm 0.016$ is inferred. For two of the points the error bars are smaller than the size of the dots.

This can be compared with values gotten with the three-dimensional Ising model: $\beta = 0.3243$ (exact) using variational approximations,[11] $\beta = 0.325 \pm 0.001$ using the n-vector model,[12] and $\beta = 0.3225 \pm 0.0001$ using high-temperature series expansion.[13] Neutron diffraction at temperature[22] gives an experimental value $\beta = 0.303 \pm 0.004$. A possible explanation of the discrepancy between this work and the neutron results lies in the fact that using quenched samples eliminates purely temperature-related effects and leaves only effects due solely to configurational differences.

V. CONCLUSIONS

The data indicate that Mössbauer results on quenched samples of FeCo show clearly the ordering transition at 730 °C and, less clearly, the 550 °C anomaly. The critical exponent β, as determined using a statistical, phenomenological model, has a value in agreement with the current theories of critical phenomena.

ACKNOWLEDGMENTS

I wish to thank Dr. D. W. Forester and Dr. S. Spooner for invaluable comments and suggestions, and Dr. H. A. Gersch and Professor P. A. Beck for helpful discussions. Financial assistance was provided by NASA Grant No. NsG-657.

[1]W. C. Ellis and E. S. Greiner, Trans. ASME 29, 415 (1941).
[2]G. Chandra, C. Bansal, and J. Ray, Phys. Status Solidi A 35, 73 (1976).
[3]P. A. Montano and M. S. Seehra, Phys. Rev. B 15, 2437 (1977).
[4]A. Narayanasamy, T. Nagarajan, P. Muthukumarasamy, and T. S. Radhakrishnan, J. Phys. F 9, 2261 (1979).
[5]B. deMayo, D. W. Forester, and S. Spooner, Bull. Am. Phys. Soc. 13, 1706 (1968); 14, 99 (1969); J. Appl. Phys. 41, 1319 (1970).
[6]B. deMayo, Ph.D. thesis (Georgia Institute of Technology, 1969) (unpublished); available from University Microfilms, Ann Arbor, Mich. 48106.
[7]J. P. Eymery and P. Moine, J. Phys. (Paris) 39, L23 (1978).
[8]G. Bayreuther and B. Lang, J. Magn. Magn. Mater. 9, 11 (1978).
[9]A. Heilmann and W. Zinn, Z. Metallkd. 58, 113 (1967).
[10]P. A. Fleury, Science 211, 125 (1981).
[11]L. P. Kadanoff, A. Houghton, and M. C. Yalabik, J. Stat. Phys. 14, 171 (1976).
[12]J. C. LeGuillo and J. Zinn-Justin, Phys. Rev. Lett. 39, 95 (1977).
13 Ye. E. Sheludyak and V. A. Rabinovich, High Temp. (USSR) 17, 40 (1979).
[14]S. Kaya and H. Sato, Phys. Math. Soc. Jpn., 3rd Series, 25, 261 (1943).
[15]H. Asano, Y. Bando, N. Nakanishi, and S. Kachi, Trans. Jpn. Inst. Met. 8, 180 (1967).
[16]T. Yokoyama, T. Takezawa, and Y. Higashida, Trans. Jpn. Inst. Met. 12, 30 (1971).
[17]H. Sato and R. Kikuchi, Acta Metall. 24, 797 (1967).
[18]J. M. Cowley, Phys. Rev. 77, 669 (1950); 120, 1648 (1960); 138, A1384 (1965).
[19]R. E. Watson, in *Hyperfine Interactions,* edited by A. J. Freeman and R. B. Frankel (Academic, New York, 1967), p. 413.
[20]B. G. Lyashenko, D. F. Litvin, I. M. Puzey, and J. G. Abov, J. Phys. Soc. Jpn. 17, 49 (1962).
[21]Reference 17; see especially Fig. 9, p. 808.
[22]J. A. Oyedele and M. F. Collins, Phys. Rev. B 16, 3208 (1977).